



Mid-wave IR signatures of CFAV Quest in the North Atlantic Summer and Winter climates

Zahir A. Daya

Daniel L. Hutt

Jeffrey Pelton

Defence R&D Canada – Atlantic

Technical Memorandum

DRDC Atlantic TM 2007-312

May 2008

This page intentionally left blank.

Mid-wave IR signatures of CFAV Quest in the North Atlantic Summer and Winter climates

Zahir A. Daya
Daniel L. Hutt
Jeffrey Pelton
Defence R&D Canada – Atlantic

Defence R&D Canada – Atlantic

Technical Memorandum

DRDC Atlantic TM 2007-312

May 2008

Principal Author

Original signed by Zahir A. Daya

Zahir A. Daya

Approved by

Original signed by Dave Hopkin

Dave Hopkin
Head/Signatures

Approved for release by

Original signed by Ron Kuwahara for

Head/Document Review Panel

© Her Majesty the Queen in Right of Canada as represented by the Minister of National Defence, 2008

© Sa Majesté la Reine (en droit du Canada), telle que représentée par le ministre de la Défense nationale, 2008

Abstract

We compare the measured and modeled mid-wave infrared signature of CFAV Quest and the maritime background during two trials Q276 and Q280. Both trials were conducted near Halifax harbour in the North Atlantic. The prevailing environmental conditions for trial Q276 were typical of North Atlantic summer (August 2003) whereas trial Q280 was carried out in a North Atlantic winter climate (February 2004). From infrared images of Quest and the maritime background, we obtain the ship, sky and sea radiances. Using the relevant environmental descriptions and an accurate geometry of Quest, we model in ShipIR the corresponding radiances. Our results show that the absolute radiances of the sea and sky background are strongly dependent on the climate and while the absolute values differ between the measurement and model predictions, the trends are consistent. There is a 20 – 40% difference in the mid-wave IR radiances of Quest between measurement and modeling. The data shows that the stack of Quest has a strongly variable radiance in the winter suggesting that it poses a great vulnerability for the ship being detected.

Résumé

Nous comparons les signatures infrarouge aux ondes moyennes modélisée et mesurée du NAFC QUEST et leurs contrastes par rapport à l'arrière-plan maritime à partir de données recueillies durant deux essais (Q276 et Q280). Les deux essais ont été menés près du port de Halifax, dans l'Atlantique Nord. Les conditions ambiantes qui prévalaient lors de l'essai Q276 représentaient bien les conditions estivales de l'Atlantique Nord (août 2003), alors que l'essai Q280 a été mené dans le climat hivernal de l'Atlantique Nord (février 2004). À partir des images infrarouge du QUEST et du contexte maritime, nous obtenons les intensités énergétiques du navire, du ciel et de la mer. À l'aide des descriptions environnementales pertinentes et d'une géométrie précise du QUEST, nous modélisons les intensités énergétiques correspondantes dans le logiciel ShipIR. Nos résultats montrent que les intensités énergétiques absolues de la mer et du ciel en arrière-plan dépendent fortement du climat et, bien que les valeurs absolues des mesures diffèrent de celles des prédictions des modèles, les tendances sont uniformes. Il y a une différence de 20 – 40% entre les intensités énergétiques infrarouge aux ondes moyennes du QUEST mesurées et modélisées. Les données montrent que la cheminée du QUEST a une intensité énergétique fortement variable en hiver, ce qui laisse supposer qu'elle pose un plus grand risque de détection du navire.

This page intentionally left blank.

Executive summary

Mid-wave IR signatures of CFAV Quest in the North Atlantic Summer and Winter climates

Zahir A. Daya, Daniel L. Hutt, Jeffrey Pelton; DRDC Atlantic TM 2007-312;
Defence R&D Canada – Atlantic; May 2008.

Background: Canadian Navy vessels operate in and transit the North Atlantic throughout the year over which the weather changes considerably. In particular, the temperature of the ocean surface has an annual variability of about 20°C. The air temperature has an even larger yearly range allowing for air-sea temperature differences that can be moderately positive in the summer and strongly negative in the winter. The vastly different summer and winter meteorological environments in the North Atlantic result in significant seasonal variation in the infrared (IR) signature of ships.

In this memorandum, we describe results from mid-wave IR measurements and modeling of the Canadian Forces Auxiliary Vessel (CFAV) Quest in North Atlantic Summer and Winter environments. The data analyzed here consisted of calibrated mid-wave IR images obtained by DRDC - Atlantic and WR Davis Engineering Limited during trials in August, 2003 and February, 2004.

Principal results: The trials comprised of several runs in which CFAV Quest cruised by the Naval Electronic and Signals Test Range Atlantic (NESTR-A) facility at Osborne head at the mouth of the Halifax harbour. Image sequences of Quest were captured with a mid-wave IR camera for several cruise configurations. Data from similar configurations between the trials are studied here to compare mid-wave IR radiances in summer and winter environments. Our results show that the summer and winter maritime environments have rather different sea and sky background radiances: the absolute radiance in the mid-wave IR changes by a factor of about two. Similarly the radiance from the ship and the contrast with the background vary between the two climates. The data support the strong variability in the radiance from the stack during the winter, less vulnerability at night than during day and comparable contrast radiances during summer and winter. This data analysis has been complemented by modeling the IR signature of Quest and its background using ShipIR, the NATO standard in ship IR signature modeling software. The modeling efforts show that the summer-winter background variation is as large as measured, and that the radiances predicted for Quest are within 20 – 40% of those measured.

Future work: Future effort should be dedicated in a more comprehensive study of ship signatures in the IR over a broader variation in the North Atlantic climate. The future trials should be designed so as to have scenarios that are stricter in configuration, between

summer and winter, than the runs that we have analyzed here. Furthermore, the trials should include a long-wave IR measurement capability. Given that the current results generally identify the stack as the region of the ship with the greater contrast radiance and radiance variability, it is important to manage the stack signature. In 2007 DRDC Atlantic attempted to control the signature of the plume (and thus indirectly that of the stack) using sea-water injection but that study was performed in the Spring. Stack cooling and reduction in the radiance fluctuations is particularly important in the Winter, a scenario to which DRDC Atlantic must extend its IR signature management efforts. The eventual goal of realizing a means to optimize the IR signature of the Canadian Navy ships is particularly pressing given the relatively greater proliferation of IR-homing threats.

Sommaire

Mid-wave IR signatures of CFAV Quest in the North Atlantic Summer and Winter climates

Zahir A. Daya, Daniel L. Hutt, Jeffrey Pelton ; DRDC Atlantic TM 2007-312 ; R & D pour la défense Canada – Atlantique ; mai 2008.

Introduction : Les navires de la marine canadienne manœuvrent dans l'Atlantique Nord et traversent cet océan toute l'année, ce qui signifie pendant des variations considérables des conditions météorologiques de l'océan. En particulier, la température de la surface de l'océan présente des fluctuations annuelles d'environ 20°C. La température de l'air a une plage encore plus grande, ce qui donne des différences de température entre l'air et la mer qui peuvent être modérément positives en été et fortement négatives en hiver. Les conditions météorologiques très différentes de l'Atlantique Nord en été et en hiver se traduisent par une importante variation saisonnière de la signature infrarouge des navires.

Dans le présent document, nous décrivons les résultats des mesures et de la modélisation de la signature infrarouge aux ondes moyennes du navire auxiliaire des Forces canadiennes (NAFC) QUEST dans les conditions estivales et hivernales de l'Atlantique Nord. Les données analysées ici consistaient en des images infrarouge étalonnées aux ondes moyennes obtenues par RDDC Atlantique et WR Davis Engineering Limited durant les essais Q276 (du 25 au 29 août 2003) et Q280 (du 15 au 18 février 2004).

Résultats : Les essais comportaient plusieurs passages au cours desquels le NAFC QUEST s'est déplacé à proximité du Centre d'essai des systèmes électroniques maritimes (NESTRA) à Osborne Head, à l'embouchure du port de Halifax. Des séquences d'images du QUEST ont été prises à l'aide d'une caméra infrarouge aux ondes moyennes pour plusieurs configurations de croisière. Des données obtenues pour des configurations semblables lors des essais Q276 et Q280 sont étudiées ici en vue d'une comparaison des intensités énergétiques infrarouge aux ondes moyennes dans des conditions estivales et hivernales. Nos résultats montrent que les conditions estivales et hivernales donnent des intensités énergétiques assez différentes de la mer et du ciel en arrière-plan : l'intensité énergétique infrarouge absolue aux ondes moyennes change d'un facteur d'environ deux. D'une façon semblable, l'intensité énergétique du navire et le contraste par rapport à l'arrière-plan varient de l'été à l'hiver. Les données viennent à l'appui de la forte variation de l'intensité énergétique de la cheminée durant l'hiver, de la vulnérabilité moindre la nuit par rapport au jour et des intensités énergétiques d'un contraste comparable en été et en hiver. Cette analyse des données a été complétée par la modélisation de la signature infrarouge du QUEST et de son arrière-plan à l'aide du logiciel ShipIR, qui constitue la norme de l'OTAN pour la modélisation assistée par logiciel des signatures infrarouge des navires.

Les efforts de modélisation montrent que la variation de l'arrière-plan de l'été à l'hiver est aussi importante que les mesures l'indiquent, et que les intensités énergétiques du QUEST présentant un écart de 20 – 40% par rapport aux intensités mesurées.

Recherches futures : Les efforts futurs devraient être déployés dans le cadre d'une étude plus exhaustive des signatures des navires dans la gamme de l'infrarouge en fonction d'une plus grande variation des conditions climatiques de l'Atlantique Nord. Les essais futurs devraient être conçus en vue de l'obtention de scénarios d'une configuration plus uniforme, en été et en hiver, que les passages que nous avons analysés ici. En outre, les essais devraient comprendre une capacité de mesure infrarouge aux ondes longues. Étant donné que les résultats disponibles permettent généralement d'identifier la cheminée comme la partie du navire ayant l'intensité énergétique d'un contraste le plus marqué et la plus grande variation de l'intensité énergétique, il est important de gérer la signature de la cheminée. Bien que RDDC Atlantique ait tenté de masquer la signature du panache (et donc indirectement celle de la cheminée) au moyen de l'injection d'eau de mer, l'étude a été menée au printemps. Le refroidissement de la cheminée et la réduction des fluctuations de l'intensité énergétique revêtent une importance particulière en hiver, scénario auquel RDDC Atlantique doit consacrer ses efforts de gestion des signatures infrarouge. L'objectif final de l'obtention d'un moyen d'optimiser la signature infrarouge des navires de la marine canadienne est particulièrement urgent, étant donné la prolifération relativement plus grande des menaces de ralliement infrarouge.

Table of contents

| | |
|--|------|
| Abstract | i |
| Résumé | i |
| Executive summary | iii |
| Sommaire | v |
| Table of contents | vii |
| List of figures | viii |
| List of tables | ix |
| 1 Introduction | 1 |
| 2 North Atlantic Summer and Winter trials | 2 |
| 3 Data Analysis | 4 |
| 3.1 Mid-wave IR radiance of the background | 4 |
| 3.2 Mid-wave IR radiances of Quest | 9 |
| 4 Ship IR signature modeling | 13 |
| 4.1 Modeling the sea and sky background | 14 |
| 4.2 Modeling Quest | 17 |
| 5 Conclusion | 20 |
| References | 22 |

List of figures

| | | |
|------------|--|----|
| Figure 1: | Map of the trial site. | 2 |
| Figure 2: | Images of CFAV Quest in the mid-wave IR from trials Q276 and Q280. | 5 |
| Figure 3: | Averaged images of the sea and sky background. | 5 |
| Figure 4: | Profiles of the mid-wave IR radiance of the sea and sky background. | 6 |
| Figure 5: | Probability distribution of temporal fluctuations in the mid-wave IR radiance of the background. | 8 |
| Figure 6: | Hull and stack regions. | 9 |
| Figure 7: | Mean mid-wave IR radiance of Quest during a run. | 12 |
| Figure 8: | Probability distribution of temporal fluctuations in the mid-wave IR radiance from the hull region of Quest. | 13 |
| Figure 9: | Model predictions of the background radiance profiles. | 15 |
| Figure 10: | Model of Quest in ShipIR. | 16 |
| Figure 11: | Model generated image of Quest in the mid-wave IR for the summer trial. | 18 |
| Figure 12: | Model generated image of Quest in the mid-wave IR for the winter trial. | 19 |

List of tables

| | | |
|----------|---|----|
| Table 1: | Configurations of IR runs. | 3 |
| Table 2: | Meteorological conditions during the runs. | 4 |
| Table 3: | Mid-wave IR radiances from the stack and hull regions. | 10 |
| Table 4: | Mid-wave IR contrast radiances from the stack and hull regions. | 11 |
| Table 5: | Parameters for the ShipIR model of the background. | 14 |
| Table 6: | Parameters for the ShipIR model of Quest. | 17 |
| Table 7: | Modeled mid-wave IR radiances from the stack and hull regions. | 18 |
| Table 8: | Modeled mid-wave IR contrast radiances from the stack and hull regions. | 19 |

This page intentionally left blank.

1 Introduction

Canadian Navy vessels operate in and transit the North Atlantic throughout the year. Most deployments begin from the Navy's east coast base in Halifax harbour entering the North Atlantic just off the Scotian shelf. Over the course of a year, the weather in the North Atlantic changes considerably. In particular, the temperature of the ocean surface has an annual variability of about 20°C. The air temperature has an even larger yearly range allowing for air-sea temperature differences that can be moderately positive in the summer and strongly negative in the winter. The vastly different summer and winter meteorological environments in the North Atlantic result in significant seasonal variation in the infrared (IR) signature of ships.

In this memorandum, we describe results from mid-wave IR measurements and modeling of the Canadian Forces Auxiliary Vessel (CFAV) Quest in North Atlantic Summer and Winter environments. The data analyzed here consisted of calibrated mid-wave IR images obtained by DRDC - Atlantic and WR Davis Engineering Limited during trials Q276 (August 25-29, 2003 [1]) and Q280 (February 15-18, 2004 [2]). Each of the trials comprised of several runs in which CFAV Quest cruised by the Naval Electronic and Signals Test Range Atlantic (NESTR-A) facility at Osborne head at the mouth of the Halifax harbour. Image sequences of Quest were captured with a mid-wave IR camera for several cruise configurations.

Data from similar configurations in trials Q276 and Q280 are studied here to compare mid-wave IR radiances in summer and winter environments. From the image data of the maritime background, we have extracted the mean mid-wave IR radiance of the sea surface, the horizon and the sky. From images of Quest, we have extracted the mid-wave IR radiance from rectangular areas on the port hull and stack. This data analysis has been complemented by modeling the IR signature of Quest and its background using ShipIR, the NATO standard in ship IR signature modeling software [3]. With ShipIR, we have modeled the summer and winter scenarios and extracted background and ship radiances for direct comparison with the trial measurements.

Our results show that the summer and winter maritime environments have rather different sea and sky background radiances: the absolute radiance in the mid-wave IR changes by a factor of about two. Similarly the radiance from the ship and the contrast with the background vary between the two climates. The data support the strong variability in the radiance from the stack during the winter, less vulnerability at night than during day and comparable contrast radiances during summer and winter. The modeling efforts show that the summer-winter background variation is as large as measured, and that the radiances of Quest are within 20 – 40% of those measured.

In Section 2 we describe the trials, the prevailing environmental conditions and the scope of the data collected. Section 3 is devoted to analyzing the data and extracting the IR

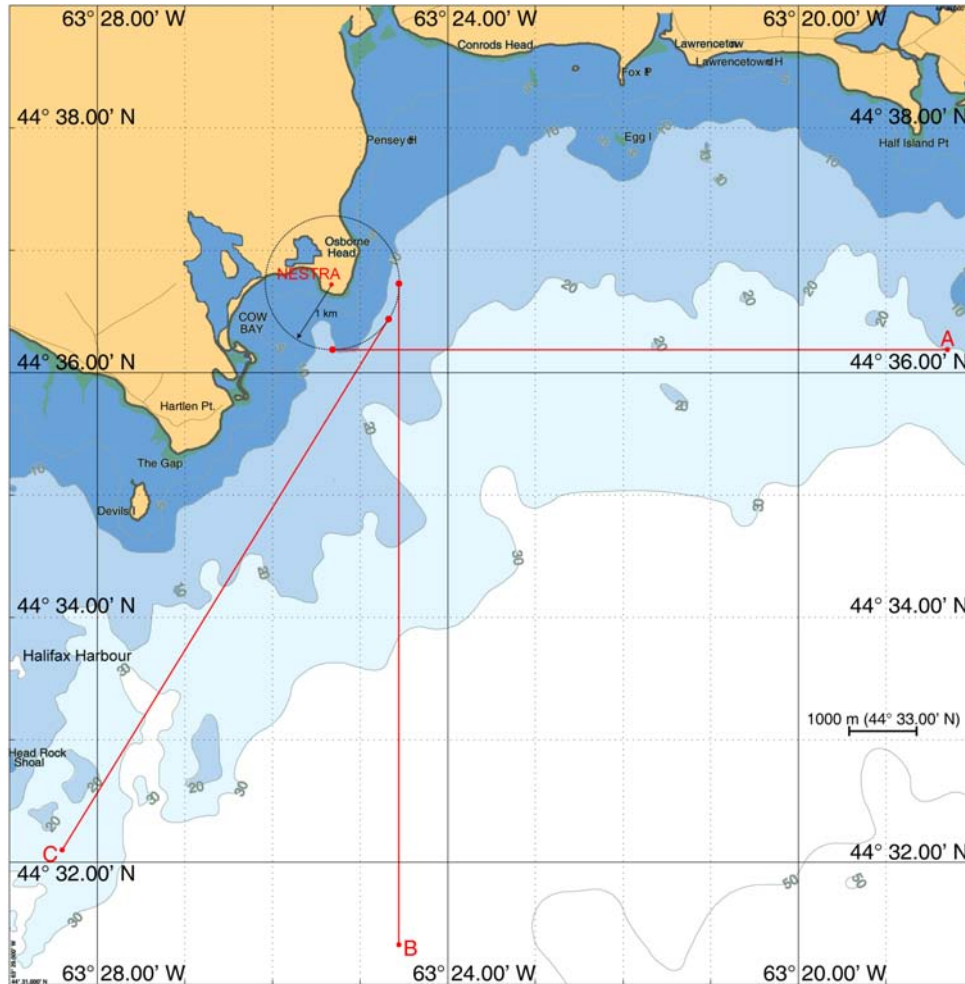


Figure 1: A map of the trial site showing the planned trajectories of the various runs and the location of the IR camera.

radiances of the ship and background regions. Modeling of the scenarios that represent these trials is described in Section 4 which includes a comparison between the measured data and model predictions. A short conclusion is given in Section 5.

2 North Atlantic Summer and Winter trials

DRDC Atlantic has a recent history in conducting sea trials to characterize and optimize the IR signature of ships using CFAV Quest as a test platform. Trials Q276 and Q280 afford an opportunity to compare the IR signature of Quest in the North Atlantic summer and winter climates. Both trials were carried out at Osborne head near the entrance to Halifax harbour. A map of the region annotated with the routes of the ship runs are shown in Fig. 1. DRDC

Table 1: Configurations of IR runs.

| trial | date | time (UTC) | run # | run type | solar azimuth | solar elevation |
|-------|--------------|---------------|----------|-------------|------------------|--------------------|
| Q276 | Aug 25, 2003 | 20:37 | 5 | B | 189.8° | 24.9° |
| | Aug 26, 2003 | 00:29 | 7A | C | 147.8° | -15.2° |
| Q280 | Feb 16, 2004 | 23:12 | 8 | C | 181.4° | -16.6° |
| | Feb 17, 2004 | 14:49 | 11 | n/a | 297.1° | 29.1° |
| | Feb 17, 2004 | 20:38 | 15 | B | 208.2° | 9.9° |
| | Feb 18, 2004 | 14:24 | 24 | n/a | 303.7° | 27.4° |

Atlantic's IR trial plan has been developed over several trials. At Osborne head, a measurement station consisting of IR cameras, blackbody sources and meteorological equipment is assembled at the NESTR-A site. Quest then cruises along predefined linear trajectories (IR-A, IR-B, IR-C and IR-D runs) past the measurement station with a distance of closest approach of about 1 km at latitude $44^{\circ}36'N$ and longitude $63^{\circ}25'W$. As Quest transits through the point of closest approach, the IR cameras are triggered to capture images of the ship and background.

The data collected during the summer trial Q276 spanned 10 runs while that from the winter trial Q280 had 26 runs [1, 2]. Comparing the run geometries, *i.e.*, Quest trajectory and solar position, we have selected the runs from the Q276 and Q280 trials that are most similar so allowing us to make as direct a comparison as is possible with these data between the summer and winter trials. In Table 1 we have listed the runs that have been selected and their configurations. Two run types, IR-B and IR-C, were found to be suitable for comparison. Trial run IR-B is northbound (heading 000°) while run IR-C is along heading 032° [4, 5]. Both runs present the port side of the ship to the IR camera at NESTR-A. The operating conditions for Quest are to cruise at a constant speed of about 10 knots under diesel-electric propulsion.

From Table 1, the IR-B runs are during day-time and allow comparison during the summer and winter climates. The solar azimuths between Q276-run-5 and Q280-run-15 differ by about 20° while the solar elevations differ by about 15° . These differences, especially in the solar elevation, are quite large, however, they present the closest day-time comparison that could be made between the Q276 and Q280 trials data. The IR-C runs are during the night about an hour after sunset when both the Q276-run-7A and Q280-run-8 have solar elevations of about -15° . Two additional winter data sets, Q280-run-11 and Q280-run-24, were studied for the background radiance: the ship was not part of the image data. These background-only data were selected because they had very cold air temperature or cloudy sky cover. In Table 2 we have summarized the meteorological conditions that were measured during the data sets that are studied in this report.

Table 2: Meteorological conditions during the runs.

| trial data set | air temperature | sea temperature | cloud cover | wind speed | wind direction | relative humidity |
|----------------|-----------------|-----------------|-------------|------------|----------------|-------------------|
| Q276-run-5 | 19.5°C | 16.0°C | clear | 6.0 m/s | 211° | 32% |
| Q276-run-7A | 14.7°C | 16.0°C | clear | 2.8 m/s | 292° | 63% |
| Q280-run-8 | -4.1°C | 0.05°C | clear | 12.1 m/s | 180° | 40% |
| Q280-run-11 | -14.4°C | 0.05°C | clear | 3.1 m/s | 180° | 65% |
| Q280-run-15 | -5.1°C | 0.05°C | clear | 3.1 m/s | 180° | 37% |
| Q280-run-24 | -5.7°C | 0.05°C | cloudy | 0.4 m/s | 210° | 75% |

Image data were acquired with a FLIR SC 1000 camera located at the NESTR-A facility at an altitude of 26 m. The mid-wave camera has a platinum-silicide sensor that functions in the spectral range of 3.24 – 5.05 μm . The focal plane array has a resolution of 248×239 pixels. The images were acquired at a rate of about 4 Hz and with a field of view of $10.1^\circ \times 9.7^\circ$. This camera has been used by DRDC Atlantic in several trials and has a properly characterized spectral response curve. It was calibrated during the summer and winter trials at the NESTR-A facility against 4 black body panels that spanned the expected range of temperatures. The slightly-nonlinear calibration curve determined by a regression analysis was used to convert the camera output signal into mid-wave IR radiances. The calibration curve is given in Ref. [2]. In Fig. 2 are shown two representative raw images from the FLIR SC 1000 camera from the day-time summer (Q276-run-5) and winter (Q280-run-15) trials. The typical data set consisted of about 20 seconds of background-only images before Quest entered the field-of-view followed by about 15 seconds of images during which Quest transits through the observation area.

3 Data Analysis

3.1 Mid-wave IR radiance of the background

The background images view the sea, horizon and sky. Since the camera is at a fixed position and has a constant field-of-view, we are imaging the same background, multiple times, over the course of a run. A single image of the background would capture some intrinsic noise, however, with several images of the same scene, we are able to average out the noise and extract the mean background. In Fig. 3 we have plotted averaged images of the backgrounds from three trial data sets: Q276-run-5 (left), Q280-run-15 (middle) and Q280-run-24 (right). The image data are in the raw camera output signal. The summer data in Fig. 3 was averaged over 74 images acquired in a 21 second duration. Note that the averaged image shows insignificant variation in the horizontal field-of-view. On the other hand, the winter data reveal a radial variation in the camera output signal and thus in the

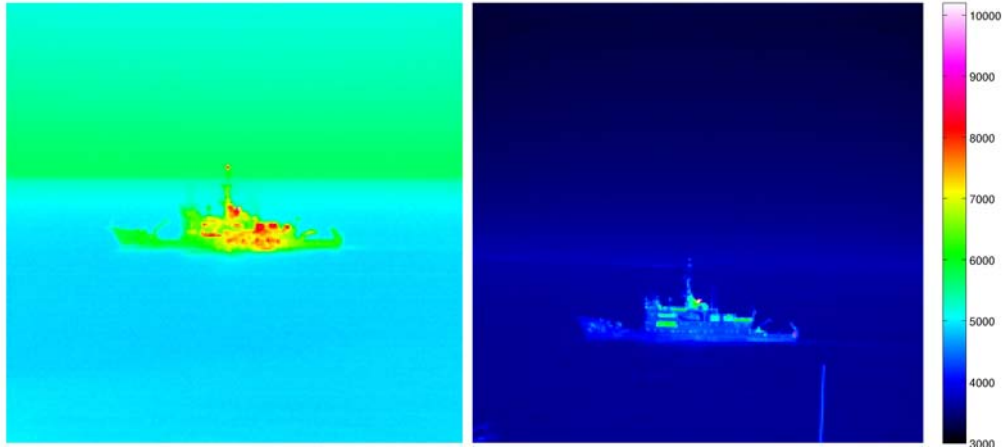


Figure 2: Representative raw images of CFAV Quest in the mid-wave IR during the summer (Q276) and winter (Q280) trials. The color bar, which spans the data range for both images, is in units of the camera output signal.

radiance. In Fig. 3 the middle image is the result of averaging 154 images that spanned about 41 seconds while the image on the right resulted from a long average of 384 images over about 12 minutes. Both these images show an unexpected radial variation and a band near the upper boundary. The systematic variation that is present in the winter and not in the summer is probably due to a thermal gradient on the camera system. The very cold winter temperatures and possibly inadequate insulation of the camera system could result in such variation. Consequently, in the analysis that follows we have restricted the data to a crop of $6^\circ \times 6^\circ$ square from the center of the image where the radial variation is imperceptible. Using this crop eliminates the band at the upper periphery and other artifacts such as the radar calibration pole seen in the middle image of Fig. 3.

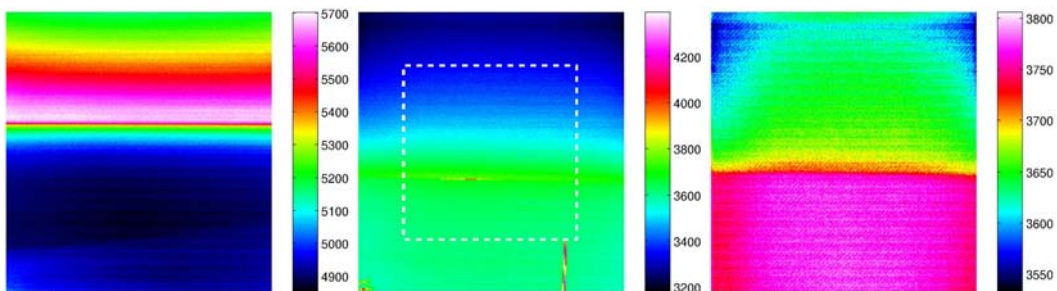


Figure 3: Averaged images of the sea and sky background from the summer trial Q276 (left), and winter trial Q280 (middle and right). The dashed line shows the $6^\circ \times 6^\circ$ square region from which data are analyzed.

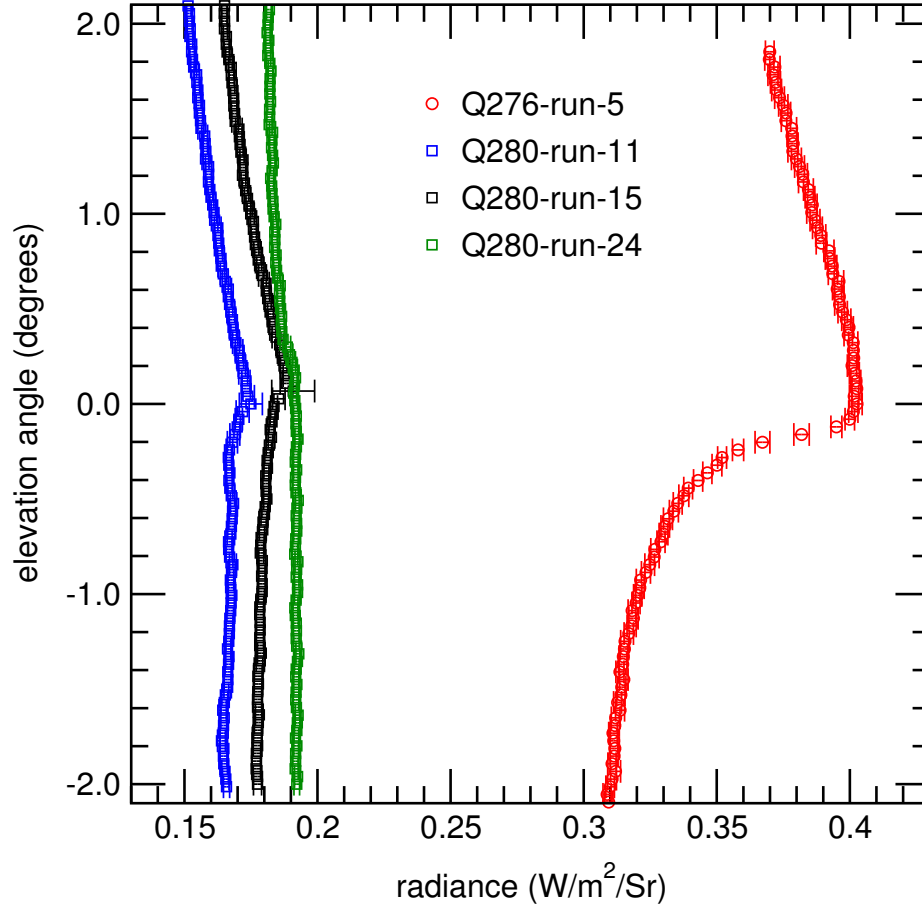


Figure 4: Profiles of the mid-wave IR radiance of the sea and sky backgrounds from the summer and winter trial data.

We now extract the mean vertical profile in the mid-wave IR radiance. Each image from a data set is cropped to the centered $6^\circ \times 6^\circ$ square which spans 149×149 pixels. Averaging over the cropped images and then over the 149 horizontal pixels results in a mean vertical or zenith profile of the mid-wave IR camera output signal (OS). The radiance (L) is obtained by applying the calibration to the OS :

$$L = (aOS + b)^c, \quad (1)$$

where a , b and c are calibration constants determined by a regression analysis to accumulated data over several calibrations [2]. The constant $c \gtrsim 1$ results in the weak nonlinearity between the camera OS and the mid-wave IR radiance L .

We always orient ourselves such that the horizon is taken to be at an elevation angle of 0° . Then negative angles span the sea and positive angles span the sky. In Fig. 4, we have plotted the radiance from the background as a function of the elevation angle for

the summer and winter trials. There are several important features in these zenith profiles. Clear sky radiances are seen to decrease, from a local maximum at the horizon, with increasing elevation angles for both the summer and winter data. The rate at which the mid-wave IR radiance decreases with the sky elevation angle is larger in the summer sky ($\sim 0.015 \text{ W/m}^2/\text{Sr}/\text{deg}$) compared to the clear winter sky ($\sim 0.01 \text{ W/m}^2/\text{Sr}/\text{deg}$). The cloudy winter sky data from Q280-run-24 shows a mild decrease in sky radiance with elevation angle at about $\sim 0.002 \text{ W/m}^2/\text{Sr}/\text{deg}$ near the horizon. This rate is much slower than the clear sky data and appears to vanish at higher elevation angles where the blanket cloud cover causes a constant radiance.

The local maximum at the horizon is common to all the zenith profiles, however, the maximum is more pronounced in the summer data than in the winter data. The peak in radiance at the horizon and its decay with sky elevation angle is often understood in terms of the decreasing line-of-sight between the sky and camera [6]. The mid-wave IR radiance from the sea approaches a constant as we look down from the horizon for small negative elevation angles. Other than the difference in the horizon and decay in the sky, the summer and winter profiles differ in absolute radiance, *i.e.*, the summer profile has an overall higher mean radiance than the winter profile. This difference is expected simply on the basis of the widely different mean temperatures in the North Atlantic summer and winter climates. The three zenith profiles from the winter data shown in Fig. 4 underline the $\sim 10\%$ variability in the background due to changes in air temperature and (associated) cloud cover over a 24 hour duration. The clouds increase the mid-wave IR radiance in the sky by their increased emission and in the sea by reflection [7].

Over short intervals in time, it is expected that the background radiance should be constant. However, the background comprises a complex physical system that is subject to many fluctuations such as sea surface roughness and atmospheric turbulence. We have used our background data to determine the distribution of fluctuations in the sea and sky radiances. Dividing a $6^\circ \times 6^\circ$ crop at the horizon, we split the data into sea and sky regions. For each region we compute the pixel-by-pixel average radiance over all the background images in the data set. We denote the average image by, for, *e.g.*, \overline{L}_{ij}^{sea} , where i and j span the pixel indices in the sea region of the image. Fluctuations about the mean or true radiance are calculated by subtracting the averaged image from individual images in the data set:

$$\Delta L_{ij}^{sea,k} = L_{ij}^{sea,k} - \overline{L}_{ij}^{sea}, \quad (2)$$

for the k^{th} image. Accumulating the fluctuations over the set of images, we compute their mean μ and standard deviation σ . We find that the mean $\mu < 10^{-6} \text{ W/m}^2/\text{Sr}$ and the standard deviation $\sigma \sim 10^{-3} \text{ W/m}^2/\text{Sr}$.

Casting the fluctuations into normal variable form:

$$\mathbf{v} = \frac{\Delta L - \mu}{\sigma}, \quad (3)$$

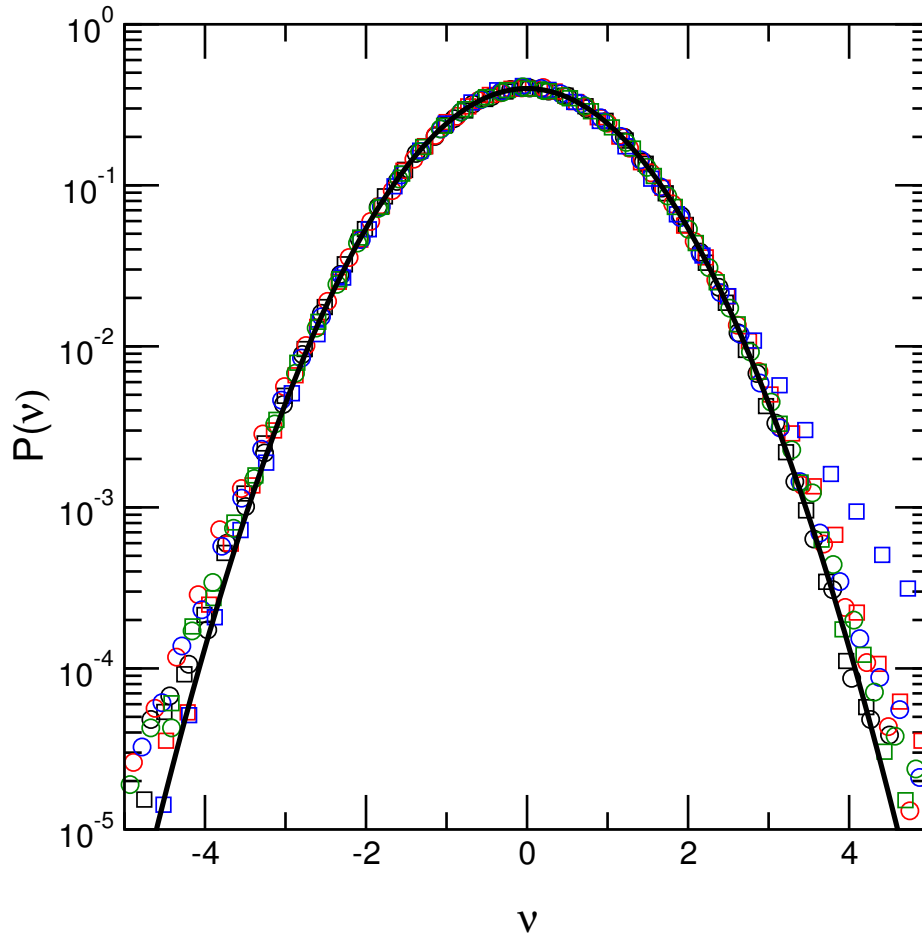


Figure 5: Probability distributions of temporal fluctuations in the mid-wave IR radiance of the sea and sky backgrounds for the summer and winter data. The symbols are data from the different runs while the solid line is the Standard Normal distribution.

we calculate the probability distribution function of the normalized (zero mean, unit standard deviation) fluctuation v with standard histogramming methods. In Eq. 3, we have suppressed the sea and sky designations.

In Fig. 5, we have plotted the probability distribution $P(v)$ for the normalized fluctuations in the sea and sky radiances for the various summer and winter runs. Typically $10^5 - 10^6$ fluctuation data were available in computing these probability distributions. We find that the radiance fluctuations are normally distributed, *i.e.*, Gaussian, for about 3 decades in probability or up to $\pm 4\sigma$. There does not appear to be any systematic variation between whether the radiance fluctuations are from the sea or sky or from winter or summer.

Two alternative methods were used to compute temporal fluctuations over short time durations. First, from consecutive images of the background, we computed the difference

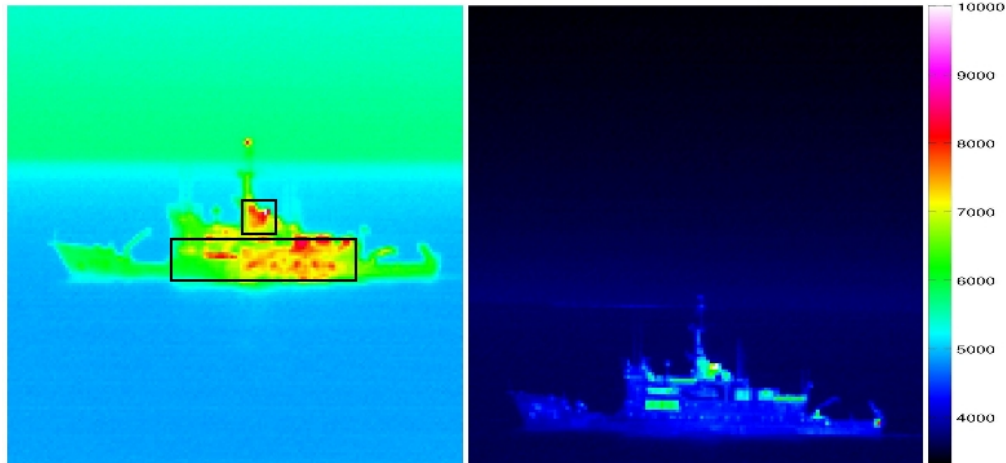


Figure 6: Cropped images from the summer (left) and winter (right) trials showing the hull and stack regions used for this study.

$\Delta L_{ij}^{sea,k} = L_{ij}^{sea,k+1} - L_{ij}^{sea,k}$. These fluctuations are over a duration of about 0.25 seconds given the approximate camera frame rate of 4 Hz. Second, we decimated the image data into consecutive sets of 4 images, averaged over each set, and then computed the difference as above between the consecutive averaged sets. These fluctuations are then over a duration of about 1 second. Casting all the fluctuations into standard normal form, we found that all the fluctuations, from the various regions and different methods, were Gaussian distributed with comparable means and variances.

3.2 Mid-wave IR radiances of Quest

Cursory observation of mid-wave IR imagery of ships from side-on show that the stack and hull have different contrasts with respect to the background. The stack has a smaller area than the hull though it stands out more prominently in images. To quantitatively study the vicinity around the stack and hull, we have defined rectangular regions fixed with respect to Quest as shown in Fig. 6. The stack region covering 8×8 pixels on the image spans an area of about 45 m^2 on Quest. The hull region, about 200 m^2 , covers the central part of the port hull with 11×47 pixels.

The IR-B and IR-C runs for Quest were studied to obtain the average properties of the mid-wave IR radiance. For each run, we identified images in the data sets that fully contained at least the stack and hull areas. From these, we extracted the stack and hull pixels. Accumulating all the stack and hull pixel data from a run, we converted the camera output signal to a radiance using the calibration in Eq. 1 and then calculated the mean μ and standard deviation σ of the radiances for the respective ship region and run. We have summarized these statistical measures in Table 3. The total number of pixel data that were used in computing

Table 3: Mid-wave IR radiances from the stack and hull regions.

| trial data set | μ_{stack} | σ_{stack} | μ_{hull} | σ_{hull} |
|----------------|----------------------|-------------------------|---------------------|------------------------|
| | W/m ² /Sr | | | |
| Q276-run-5 | 0.65 | 0.10 | 0.61 | 0.06 |
| Q276-run-7A | 0.44 | 0.10 | 0.36 | 0.01 |
| Q280-run-8 | 0.22 | 0.28 | 0.16 | 0.01 |
| Q280-run-15 | 0.48 | 0.66 | 0.27 | 0.05 |

the statistics are about 2000 per run for the stack region and about 16000 per run for the hull region. Several inferences can be reached by studying Table 3. Independent of climate, the stack has a greater mean mid-wave IR radiance than the hull. This difference is larger in the winter than in the summer. The mid-wave IR radiances, mean and standard deviations, are generally greater during the day than at night for both the summer and winter climates.

In comparing the role of the climate, we compare Q276-run-5 with Q280-run-15 for the day-time case and Q276-run-7A with Q280-run-8 for the night-time case. For the day and night, the winter stack and hull have lower mean radiances than in the summer. However, the standard deviations of the mid-wave IR radiance in the winter stack, during day and night, are much greater than in the summer. Overall, the standard deviations in the mid-wave IR radiance from the hull are comparatively small compared to those from the stack. The probable reason for this is the largely isothermal state of the hull which since it is in contact with the water is buffered from thermal swings due to the immense heat capacity of the ocean. The stack being exposed to air motion is rather subject to rather large local variations in wind, air temperature and humidity.

While radiance statistics are important, it is the difference between the ship and the background radiances that is critical for detection. This difference, termed a contrast radiance, is often referred to as the IR signature of a ship. For the observations from Osborne head, the ship is contrasted against the sea background. This is expected to be the case for most side-on observations of ships. Here we contrast the mean stack and hull radiances against the sea background. Recall that the mid-wave IR radiance from the sea background is quite constant (see Fig. 4). We use the sea radiance averaged over -1° to -2° in elevation angle, $\overline{L_{\text{sea}}}$, to compute the mean mid-wave IR contrast:

$$C_{\text{stack,hull}} = \mu_{\text{stack,hull}} - \overline{L_{\text{sea}}} . \quad (4)$$

The contrast, by itself, is not sufficient in gauging the likelihood of detection. For example the same contrast can be obtained by uniformly scaling all the radiances. So we must augment the contrast with a measure that compares the signature to an intrinsic variable. Often, one uses the ratio of the contrast to the noise equivalent radiance of the sensor.

Table 4: Mid-wave IR contrast radiances from the stack and hull regions.

| trial data set | C_{stack} | R_{stack} | C_{hull} | R_{hull} |
|----------------|----------------------|--------------------|----------------------|-------------------|
| | W/m ² /Sr | | W/m ² /Sr | |
| Q276-run-5 | 0.34 | 1.10 | 0.30 | 0.97 |
| Q276-run-7A | 0.12 | 0.38 | 0.04 | 0.13 |
| Q280-run-8 | 0.05 | 0.29 | -0.01 | -0.06 |
| Q280-run-15 | 0.30 | 1.67 | 0.09 | 0.50 |

Alternatively, one may assess a different intrinsic noise level from the background scene. Here, we simply consider the ratio between the contrast and the background radiance:

$$R_{\text{stack,hull}} = \frac{C_{\text{stack,hull}}}{L_{\text{sea}}} = \frac{\mu_{\text{stack,hull}}}{L_{\text{sea}}} - 1, \quad (5)$$

in assessing the extent to which the contrast differs from the background.

In Table 4 we have listed the contrast radiances and contrast-to-background ratios for the stack and hull regions from the 4 Quest runs that we have studied. The contrasts, which are generally larger for the stack than for the hull, are greater during the day than during the night. The winter day and night contrasts are smaller than in the summer. However, the contrast-to-background ratios which measure the fraction by which the contrasts exceed the background suggest that the most significant signature is from the stack on the winter day. Night time contrast-to-background ratios are much smaller than their day time counterparts. This implies that signature management techniques should address day time stack and hull IR signatures.

In our trials, Quest is usually imaged over a period of about 10 – 15 seconds. Parameters for the large-scale environment are constant over such short durations, however, local changes in thermal load may occur such as those caused by atmospheric turbulence or deviations in engine power. To assess the temporal stability of the mid-wave IR radiance of Quest, we have studied the mean radiance from the stack and hull as a function of time, *i.e.*, a consecutive sequence of images. In Fig. 7 we have plotted the mean mid-wave IR radiance of Quest as a function of time for a winter and summer run.

All the mid-wave IR radiances from Quest are essentially constant in time except for the winter stack which shows large fluctuations. These are also noted in the significantly larger standard deviations of the stack radiances given in Table 3. The large fluctuations are probably due to local meso-scale atmospheric turbulence such as coherent pockets or vortices of colder or warmer air etc.

Whereas the mean radiances of the hull regions are quite constant over a sequence of consecutive images for time scales of about 10 seconds, the pixel-by-pixel fluctuations have a

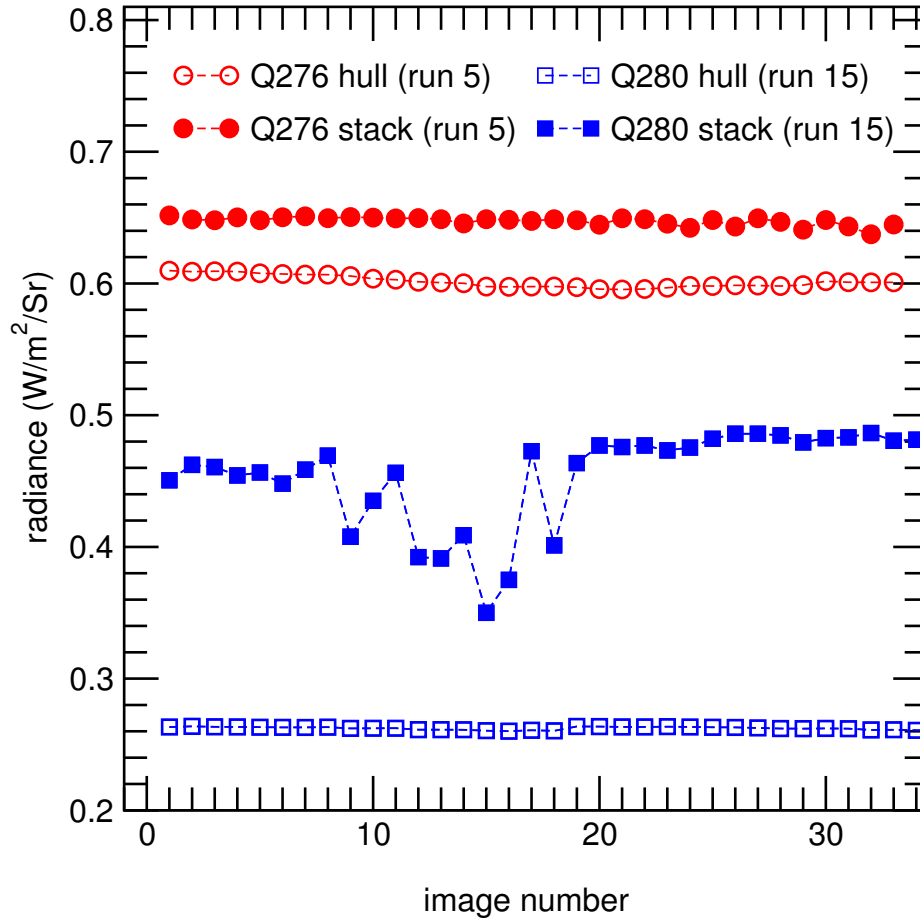


Figure 7: The mean mid-wave IR radiances of the hull and stack regions in the summer (Q276) and winter (Q280) trials.

greater variability. As with the sea and sky backgrounds, we have computed the probability distribution of the normalized fluctuations in the hull radiances for the winter and summer runs. In brief, fluctuations are the differences between the averaged hull image and individual frames. These are collected and cast into a standard normal variable, v , by subtracting a mean $\sim 10^{-4} \text{ W/m}^2/\text{Sr}$ and dividing by the standard deviation $\sim 10^{-2} \text{ W/m}^2/\text{Sr}$. Histogramming the normalized fluctuations, we have calculated the probability distribution $P(v)$ which is plotted in Fig. 8. The probability distributions, which are based on about 16000 data, are not Gaussian but rather more like generalized exponentials with fatter-than-gaussian tails. Recall that the fluctuations in the sea and sky background radiances were decidedly Gaussian. Fluctuations from the stack were not characterized since there are insufficient data since the stack only spans 8×8 pixels.

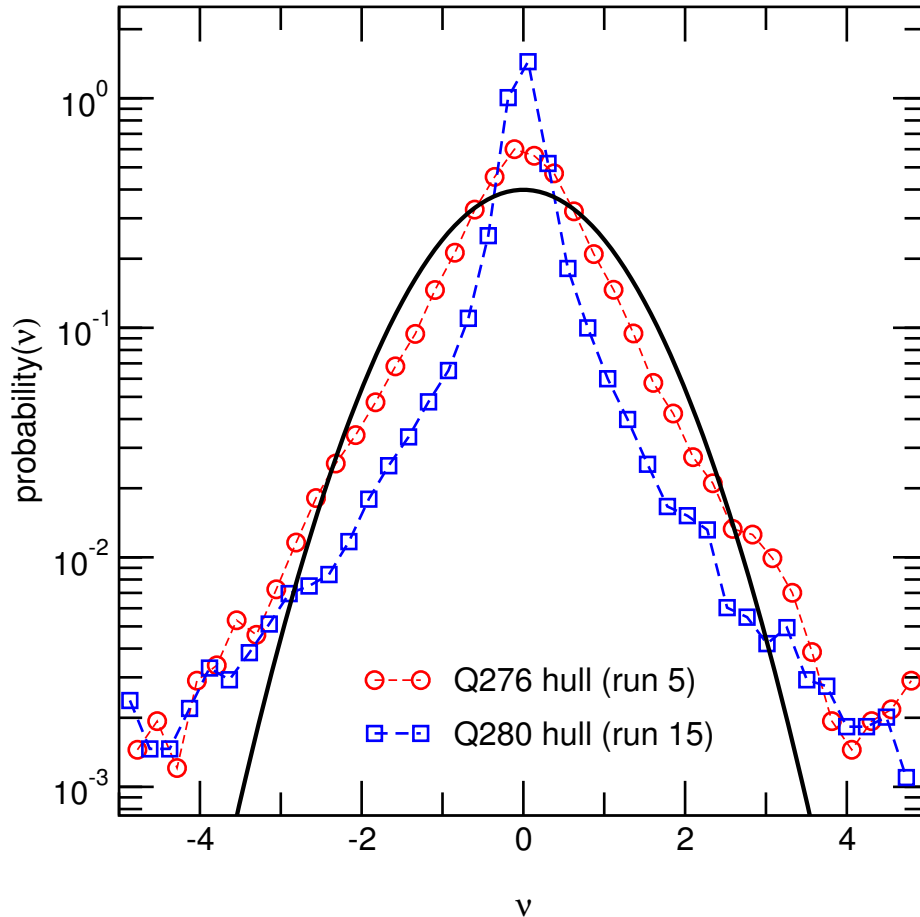


Figure 8: Probability distribution of temporal fluctuations in the mid-wave IR radiance from the hull region of Quest from the summer and winter trials. The solid line is a standard normal probability distribution.

4 Ship IR signature modeling

Modeling the IR signature of a ship is a daunting task. It encompasses modeling the sea and sky backgrounds, the ship's surface and thermal conditions, and the intervening atmosphere between the ship and sensor. We use ShipIR, a commercial code developed by W. R. Davis Engineering Limited [3] to model the IR signature of Quest. ShipIR, which was initially developed under contract from DRDC Valcartier in 1992, has over the years evolved into the state-of-the-art for modeling ships in the IR, being designated as the NATO standard in 1995. ShipIR consists a user-interface to a collection of sub-models to compute and graphically display the IR radiance of the sea, sky and ship as seen by an observer. Below, we briefly describe how the ShipIR model was computed for the day time winter and summer trials.

Table 5: Parameters for the ShipIR model of the background.

| trial data set | Q276-run-5 / Q280-run-15 |
|----------------------------|---|
| atmospheric model | mid-latitude summer / mid-latitude winter |
| boundary layer | navy maritime |
| air mass parameter | 8 |
| cloud model | no clouds or rain |
| average wind speed | 5.1 / 3.1 m/s |
| latitude | 44.6°N |
| longitude | 63.4°W |
| number of zenith points | 18 |
| number of azimuth points | 36 |
| sky type | lowmodtran |
| sea type | shaw |
| sea glint | normal |
| sun type | lowmodtran |
| scattering | multiple |
| observer altitude | 26 m |
| observer IR band | 3.2362-5.0505 μm |
| observer spectral response | FLIR SC 1000 filter |

4.1 Modeling the sea and sky background

In ShipIR, the background is specified by the geographical location, the time of day, the prevailing atmospheric conditions, and the state of the sea. From the time of day and the location (latitude, longitude) ShipIR determines the solar elevation and azimuth. The atmospheric conditions, most of which are given in Table 2, determine the sea and sky temperatures and more importantly scale the standard atmospheric profiles that are used in calculating the transmission of IR radiation through the atmosphere. Certain physical models for the sea surface (Shaw-Churnside, Cox and Munk etc) can be selected in ShipIR.

Computational parameters such as mesh densities and numerical convergence criteria can be controlled in ShipIR. In processing the background, ShipIR requires the position and spectral characteristics of an observer. Each background is computed with respect to an observer. In trials Q276 and Q280, the observer is a mid-wave IR FLIR SC 1000 camera with a well-characterized spectral response. In Table 5 we have listed the parameters (except the solar position given in Table 1 and the meteorological variables that are given in Table 2) that were used in computing the model backgrounds for trials Q276-run-5 and Q280-run-15. Transmission calculations of the IR radiation in ShipIR is routed to the, user-selected, standard LOWTRAN [8] or MODTRAN [9] code. We have used the MODTRAN option for all the processing in ShipIR.

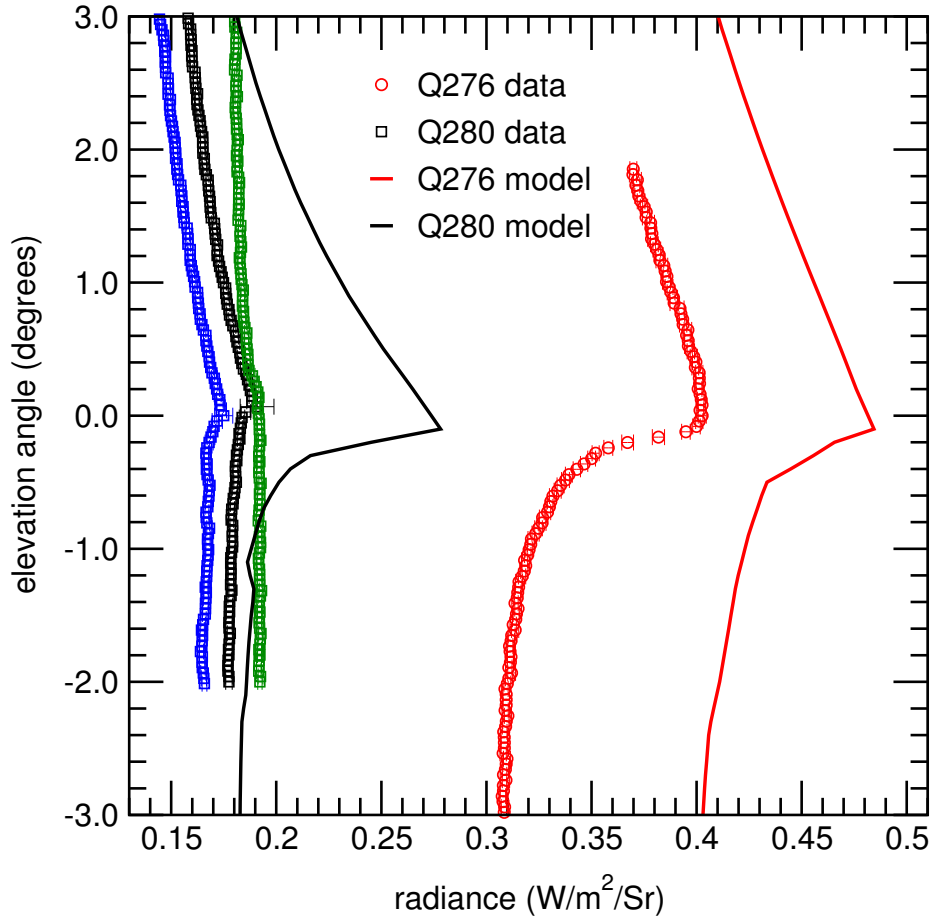


Figure 9: The model prediction of the radiance profile of the sea and sky background for the summer and winter scenarios. Also shown are the measured data.

Once computed, the background model in ShipIR can be analyzed to extract the mid-wave IR radiance of the sea and sky. These are stationary model results, *i.e.*, the background radiances are constant since the background is computed at a single instance in time. The data, on the other hand, were acquired over 20 second durations and contain fluctuations as discussed in Section 3. Since ShipIR is based on a deterministic, time-independent set of equations, it does not calculate the temporal stochastic variation in the sea and sky backgrounds. Thus the only suitable comparison between the background data and the model is in the mean sea and sky radiances. These are conveniently characterized in the zenith profiles which plot the background radiance versus the elevation angle.

Routines provided within the ShipIR package can be used to extract the zenith profile of the background at a given observer viewing angle and for range of elevation angles. We have plotted the model predictions of the mid-wave IR background radiance as a function of elevation angle for the summer (Q276-run-5) and winter (Q280-run-15) cases in Fig. 9. On

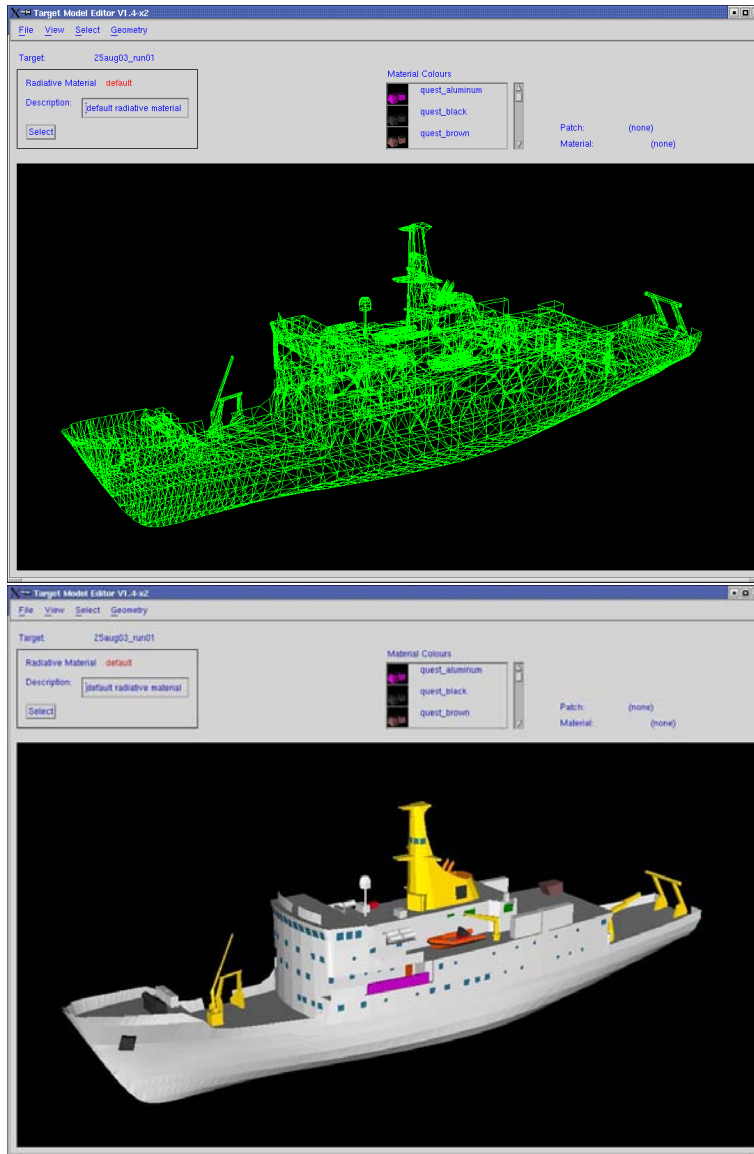


Figure 10: The 3D CAD and surface property model of Quest in ShipIR.

the same plot, we have also shown the mid-wave IR radiances that were obtained from the image data collected during the trials. Whereas, the overall features in the zenith profiles between data and model are similar there are crucial differences.

The summer data and model have the same general shape. There appears to be a large offset in radiance with the model over-predicting the sea radiance by about $0.1 \text{ W/m}^2/\text{Sr}$ at shallow angles. However, the model over-prediction is smaller for the sky and thus the

mismatch between the model and the data is not simply a uniform offset. For the winter case, the model and data differ significantly near the horizon. The model predicts a strong local maximum, comparable to that in the summer, at the horizon. The data, however, have a weak local maximum at the horizon. Directly comparing the sea radiances between model and data, we see that the model over-predicts by about $0.01 \text{ W/m}^2/\text{Sr}$ with larger differences for shallow elevation angles in the sky. The summer (winter) over-predictions of the sea radiance by about 30% (5%) will inevitably lead to errors in the model predictions for the IR contrast between the ship and sea.

4.2 Modeling Quest

The Quest model in ShipIR has been developed over the past few years by W. R. Davis Engineering Limited under contract from DRDC Atlantic [2]. The model consists of a 3D CAD geometry, surface optical properties and thermal boundary conditions. The model geometry “quest”, shown in Fig. 10, has about 7000 oriented patches to make an accurate geometrical representation of the ship. The external facing surfaces of the patches are assigned the material properties that correspond to the ship’s surface. These properties include the solar absorptivity, the emissivity and reflectivity in narrow spectral regions spanning the IR bands and the solar spectrum. For Quest, the collection of surface properties that are used by ShipIR in our modeling effort for this manuscript, are termed “simvex”. The thermal model consists of thermal boundary conditions on temperature controlled spaces, and of the composition, mass flux and temperature of the exhaust flue. These are collective known as “mp-runs” corresponding to the appropriate parameters for Quest under diesel-electric propulsion. Both the “simvex” and “mp-runs” input values have been generated by W. R. Davis Engineering Limited. In Table 6, we have listed most of the parameter inputs into the target model of ShipIR.

Table 6: Parameters for the ShipIR model of Quest.

| trial data set | Q276-run-5 / Q280-run-15 |
|-----------------------------|--------------------------|
| geometry | quest |
| materials | simvex |
| spectral analysis | full spectral |
| plume | mp-runs |
| thermal boundary conditions | mp-runs |
| multi-bounce BRDF | on |
| bi-directional BRDF | on |
| speed | 5.55 m/s |
| position (x,y,z) | (0,0,-5) m |
| yaw, pitch, roll | 90(North), 0,0 |

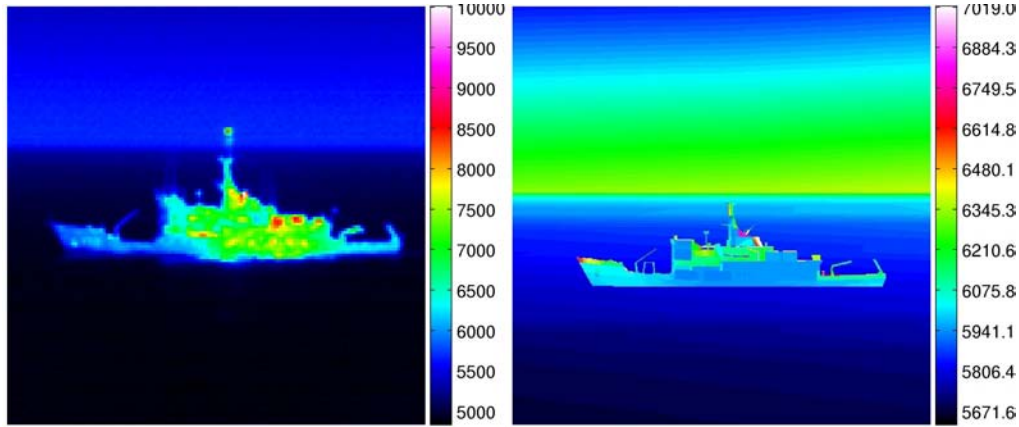


Figure 11: Images in the mid-wave IR of Quest from the data (left) and generated by the modeling (right) for the summer trial. The color bar is in units of the object signal.

The geometry “quest” representing Quest is placed at the origin. The negative z coordinate ensures that the vessel has the appropriate water line. The Quest cruises northwards at about 10 knots without any roll or pitch at the instant that the model is evaluated. In our modeling, ShipIR has been set to use the bi-direction reflectance distribution function for the various painted surfaces. Once again, we have selected MODTRAN for all the transmission calculations when processing the target in the background. The target specified in Table 6 is processed in the summer and winter backgrounds to calculate the IR radiance of Quest. Once completed, the observer’s view is rendered in the ShipIR graphical interface.

In Figs. 11 and 12, we have shown images of Quest from the data and those predicted by the model for the Q276-run-5 (summer) and Q280-run-15 (winter) cases. Qualitatively, the model and data are generally alike. Visually assessing the contrasts between the ship and the sea, it is apparent that in the summer the data has a higher contrast than the model while in the winter the reverse is true. To compare the model and data quantitatively, we have analyzed the modeled ship for mid-wave IR radiance from the stack and hull regions. Our results are summarized in Table 7.

Comparing the radiances from the trial data (Table 3) with those modeled with ShipIR (Table 7), we note that the model underpredicts the summer data and overpredicts the

Table 7: Modeled mid-wave IR radiances from the stack and hull regions.

| model | μ_{stack} | σ_{stack} | μ_{hull} | σ_{hull} |
|-------------|----------------------|-------------------------|---------------------|------------------------|
| | W/m ² /Sr | | | |
| Q276-run-5 | 0.43 | 0.17 | 0.41 | 0.12 |
| Q280-run-15 | 0.53 | 0.23 | 0.56 | 0.17 |

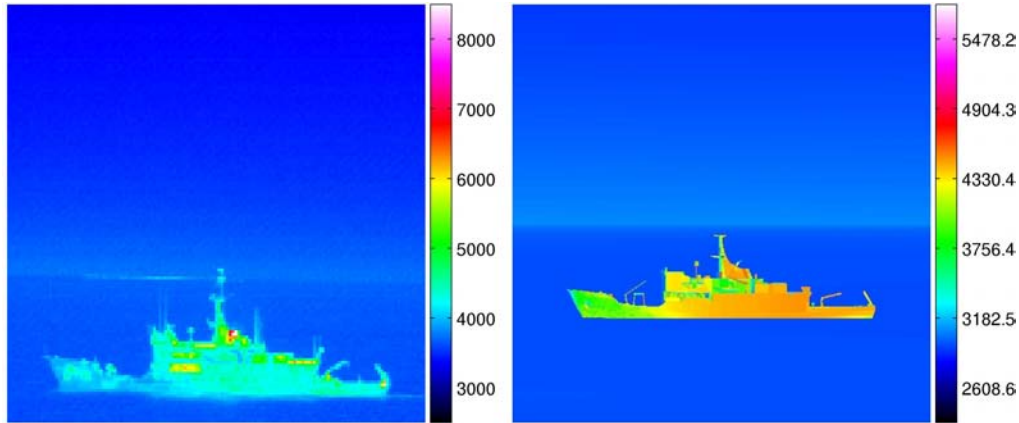


Figure 12: Images in the mid-wave IR of Quest from the data (left) and generated by the modeling (right) for the winter trial. The color bar is in units of the object signal.

winter data. The data and model differ by about 20 – 40% for the two runs. The model has larger standard deviation in the predicted radiance for the hull region than is present in the data. The measured radiances from the stack during the winter have a significantly greater standard deviation than the those modeled in ShipIR.

Contrast radiances against the sea background are computed from the ShipIR models in the same manner as for the data described in Section 3.2. We use Eqs. 4 and 5 applied to the ShipIR model results to calculate the stack and hull contrasts. Our results are given in Table 8. The summer (Q276-run-5) day time case has very small mid-wave IR radiance contrast in the model. This is because the model overpredicts the radiance of the sea background and underpredicts the radiances from the ship. Both effects conspire to result in an unusually poor contrast. Had the background been properly predicted, the contrast ratios would have been an order of magnitude larger. In the winter (Q280-run-15) day time case, the contrast and contrast ratio for the stack is in reasonable agreement with the data. The radiance from the winter sea and from the ship stack is approximately the same between the model and the data. However, the radiance from the ship hull are quite different between the model and the data resulting in much larger model contrast and contrast ratio. It is not clear why the hull radiance is overpredicted by the model.

Table 8: Modeled mid-wave IR contrast radiances from the stack and hull regions.

| model | C_{stack} | R_{stack} | C_{hull} | R_{hull} |
|-------------|----------------------|--------------------|----------------------|-------------------|
| | W/m ² /Sr | | W/m ² /Sr | |
| Q276-run-5 | 0.02 | 0.04 | -0.01 | -0.01 |
| Q280-run-15 | 0.34 | 1.82 | 0.37 | 1.98 |

5 Conclusion

The wide range of maritime climatic conditions in the North Atlantic strongly influences the mid-wave IR signature of ships operating in the region. Most of DRDC Atlantic's research efforts in the IR signature of ships have been during late Spring to mid-Summer when we periodically range Quest and test IR signature management equipment. One trial during almost severe winter conditions was carried out in trial Q280. With the political emphasis on Canadian sovereignty in the Arctic and the subsequent need to maintain a northern defense capability, DRDC Atlantic is advised to undertake future cold-water IR signature studies of ships.

Our initial study in comparing mid-wave IR radiances of the summer and winter maritime backgrounds and of Quest is mildly oblique in that the data sets are rather small and the conditions under which the comparisons are made are only approximately the same, *e.g.*, the solar elevations between the summer and winter day time runs differ by about 15°. A more rigorous planning of ship runs vis-a-vis the orientation of thermal and radiological sources. Nevertheless, our brief comparison between prior summer and winter mid-wave IR image data of Quest show that the radiances are strongly variable between the two climatic conditions.

The mid-wave IR radiances of the backgrounds increase by a factor of almost two from the winter to the summer in both the trial measurements and the ShipIR modeling. There is considerable variability in the backgrounds over the course of a few hours during which air temperature and cloud cover change. As yet, irreconcilable differences between the measured and modeled backgrounds remain: the summer day time modeled background mid-wave IR radiance is systematically too high at all elevation angles and the radiance at the horizon peaks too strongly in the modeled winter day time case.

The measurements of Quest show that the mid-wave IR radiance from the stack region exceed those from the hull region. The variation in the hull region is significantly less than in the stack region, especially in the winter when the stack radiances fluctuate strongly. Results from the model, while not inconsistent with the measurements, do not clearly substantiate the stack-greater-than-hull radiances or the low variability in hull radiance. From the two day-time summer and winter runs, we find that the model underpredicts the ship radiances in the summer and overpredicts them in the winter. Measured contrast radiances and contrast ratios of the hull and stack regions against the sea background show that the stack presents the greatest vulnerability for the ship especially in the winter. The modeled contrasts and contrast ratios support the large winter vulnerability but suggest a summer vulnerability that is surprisingly modest.

Future effort should be dedicated in a more comprehensive study of ship signatures in the IR over a broader variation in the North Atlantic climate. The future trials should be designed with obtaining scenarios that are stricter in configuration than the runs that we

have analyzed here. Furthermore, the trials should include a long-wave IR measurement capability. Given that the current results generally identify the stack as the region of the ship with the greater contrast radiance and radiance variability, it is important to manage the stack signature. While DRDC Atlantic has attempted to control the signature of the plume (and thus indirectly that of the stack) using sea-water injection, the study has been performed in the Spring [10]. Stack cooling and reduction in the radiance fluctuations is particularly important in the Winter, a scenario to which DRDC Atlantic must extend its IR signature management efforts.

References

- [1] Vaitekunas, D. A. (2004), Infrared signature instrumentation, measurement and modelling of CFAV Quest for Trial Q-276, *Document number A320-001, Rev 0*.
- [2] Vaitekunas, D. A. (2005), Infrared signature instrumentation, measurement and modelling of CFAV Quest for Trial Q-280, *Document number A330-001, Rev 0*.
- [3] D.A. Vaitekunas (2002), Technical Manual for ShipIR/NTCS (v2.9), Release Notes (v3.2).
- [4] Hutt, D. L. (2003), Trials plan for CFAV Quest trial Q-276.
- [5] Hutt, D. L. (2005), Trials plan for CFAV Quest trial Q-280.
- [6] Mermelstein, M. D. (1994), Midwave and long-wave infrared radiance and clutter at the ocean-sky horizon, *Optical Society of America, Vol. 19, No. 18*.
- [7] M.A. Goforth, G. W. Gilchrist & J.D. Sirianni (2002), Cloud effects on thermal downwelling sky radiance, *SPIE Thermosense Conference Proceedings*.
- [8] Air Force Research Laboratories, Space Vehicles Directorate (AFRL/VSBT)., LOWTRAN - Low spectral resolution atmospheric transmittance algorithm and computer model.
- [9] Air Force Research Laboratories, Inc., Space Vehicles Directorate (AFRL/VSBT) in collaboration with Spectral Sciences, MODTRAN - Moderate spectral resolution atmospheric transmittance algorithm and computer model.
- [10] Hutt, D. L. (2007), Trials plan for CFAV Quest trial Q-305.

Distribution list

DRDC Atlantic TM 2007-312

Internal distribution

- 2 Authors
Attn: Zahir A. Daya, Daniel L. Hutt
- 5 Library

Total internal copies: 7

External distribution

Department of National Defence

- 1 DRDKIM
NDHQ/DRDKIM
- 1 DSTM
NDHQ/DSTM
- 1 DSTM 3
NDHQ/DSTM 3
Attn: Greg Walker
- 2 DMSS 2
NDHQ/DMSS 2
Attn: Jan Czaban, Ping Kwok
- 2 DRDC Ottawa
3701 Carling Avenue, Ottawa, Ontario, K1A 0Z4
Attn: Satish Kayshap, Stephane Legault
- 3 DRDC Valcartier
2459 Pie-XI Blvd North, Qubec, Quebec G3J 1X5
Attn: Francoise Reid, Luc Forand, Denis Dion

Other Canadian recipients

- 1 David A. Vaitekunas
Senior Development Engineer
W.R. Davis Engineering Ltd

1260 Old Innes Road
Ottawa, Ontario
CANADA K1B 3V3

International recipients

- 1 Douglas Fraedrich
Naval Research Laboratory
Attn: Code 5757
4555 Overlook Ave., SW
Washington, DC 20375-5339 USA

- 1 Keith Youern
Defence Scientific and Technology Laboratory (Dstl)
Room C121 East Court, Portsdown West
Portsdown Hill Road
Fareham, Hants P017 6AD, England

Total external copies: 13

Total copies: 20

DOCUMENT CONTROL DATA

(Security classification of title, body of abstract and indexing annotation must be entered when document is classified)

| | | |
|--|---|--|
| <p>1. ORIGINATOR (The name and address of the organization preparing the document. Organizations for whom the document was prepared, e.g. Centre sponsoring a contractor's report, or tasking agency, are entered in section 8.)</p> <p>Defence R&D Canada – Atlantic P.O. Box 1012, Dartmouth, Nova Scotia, Canada B2Y 3Z7</p> | <p>2. SECURITY CLASSIFICATION (Overall security classification of the document including special warning terms if applicable.)</p> <p>UNCLASSIFIED</p> | |
| <p>3. TITLE (The complete document title as indicated on the title page. Its classification should be indicated by the appropriate abbreviation (S, C or U) in parentheses after the title.)</p> <p>Mid-wave IR signatures of CFAV Quest in the North Atlantic Summer and Winter climates</p> | | |
| <p>4. AUTHORS (Last name, followed by initials – ranks, titles, etc. not to be used.)</p> <p>Daya, Z.A.; Hutt, D.L.; Pelton, J.</p> | | |
| <p>5. DATE OF PUBLICATION (Month and year of publication of document.)</p> <p>May 2008</p> | <p>6a. NO. OF PAGES (Total containing information. Include Annexes, Appendices, etc.)</p> <p>38</p> | <p>6b. NO. OF REFS (Total cited in document.)</p> <p>10</p> |
| <p>7. DESCRIPTIVE NOTES (The category of the document, e.g. technical report, technical note or memorandum. If appropriate, enter the type of report, e.g. interim, progress, summary, annual or final. Give the inclusive dates when a specific reporting period is covered.)</p> <p>Technical Memorandum</p> | | |
| <p>8. SPONSORING ACTIVITY (The name of the department project office or laboratory sponsoring the research and development – include address.)</p> <p>Defence R&D Canada – Atlantic P.O. Box 1012, Dartmouth, Nova Scotia, Canada B2Y 3Z7</p> | | |
| <p>9a. PROJECT NO. (The applicable research and development project number under which the document was written. Please specify whether project or grant.)</p> <p>11GS</p> | <p>9b. GRANT OR CONTRACT NO. (If appropriate, the applicable number under which the document was written.)</p> | |
| <p>10a. ORIGINATOR'S DOCUMENT NUMBER (The official document number by which the document is identified by the originating activity. This number must be unique to this document.)</p> <p>DRDC Atlantic TM 2007-312</p> | <p>10b. OTHER DOCUMENT NO(s). (Any other numbers which may be assigned this document either by the originator or by the sponsor.)</p> | |
| <p>11. DOCUMENT AVAILABILITY (Any limitations on further dissemination of the document, other than those imposed by security classification.)</p> <p><input checked="" type="checkbox"/> Unlimited distribution</p> <p><input type="checkbox"/> Defence departments and defence contractors; further distribution only as approved</p> <p><input type="checkbox"/> Defence departments and Canadian defence contractors; further distribution only as approved</p> <p><input type="checkbox"/> Government departments and agencies; further distribution only as approved</p> <p><input type="checkbox"/> Defence departments; further distribution only as approved</p> <p><input type="checkbox"/> Other (please specify):</p> | | |
| <p>12. DOCUMENT ANNOUNCEMENT (Any limitation to the bibliographic announcement of this document. This will normally correspond to the Document Availability (11). However, where further distribution (beyond the audience specified in (11)) is possible, a wider announcement audience may be selected.)</p> | | |

13. ABSTRACT (A brief and factual summary of the document. It may also appear elsewhere in the body of the document itself. It is highly desirable that the abstract of classified documents be unclassified. Each paragraph of the abstract shall begin with an indication of the security classification of the information in the paragraph (unless the document itself is unclassified) represented as (S), (C), (R), or (U). It is not necessary to include here abstracts in both official languages unless the text is bilingual.)

We compare the measured and modeled mid-wave infrared signature of CFAV Quest and the maritime background during two trials Q276 and Q280. Both trials were conducted near Halifax harbour in the North Atlantic. The prevailing environmental conditions for trial Q276 were typical of North Atlantic summer (August 2003) whereas trial Q280 was carried out in a North Atlantic winter climate (February 2004). From infrared images of Quest and the maritime background, we obtain the ship, sky and sea radiances. Using the relevant environmental descriptions and an accurate geometry of Quest, we model in ShiplR the corresponding radiances. Our results show that the absolute radiances of the sea and sky background are strongly dependent on the climate and while the absolute values differ between the measurement and model predictions, the trends are consistent. There is a 20 – 40% difference in the mid-wave IR radiances of Quest between measurement and modeling. The data shows that the stack of Quest has a strongly variable radiance in the winter suggesting that it poses a great vulnerability for the ship being detected.

14. KEYWORDS, DESCRIPTORS or IDENTIFIERS (Technically meaningful terms or short phrases that characterize a document and could be helpful in cataloguing the document. They should be selected so that no security classification is required. Identifiers, such as equipment model designation, trade name, military project code name, geographic location may also be included. If possible keywords should be selected from a published thesaurus. e.g. Thesaurus of Engineering and Scientific Terms (TEST) and that thesaurus identified. If it is not possible to select indexing terms which are Unclassified, the classification of each should be indicated as with the title.)

infrared signatures
mid-IR, mid wave
signature management
infrared sensors
infrared radiance

This page intentionally left blank.

Defence R&D Canada

Canada's leader in defence
and National Security
Science and Technology

R & D pour la défense Canada

Chef de file au Canada en matière
de science et de technologie pour
la défense et la sécurité nationale



www.drdc-rddc.gc.ca